Available online at www.sciencedirect.com
ScienceDirect
Renewable Energy 33 (2008) 780–790
RENEWABLE ENERGY
www.elsevier.com/locate/renene

Technical Note

Design and performance prediction of a novel double heat pipes type adsorption chiller for fishing boats

K. Wang, J.Y. Wu*, Z.Z. Xia, S.L. Li, R.Z. Wang

Institute of Refrigeration and Cryogenics, Shanghai Jiao Tong University, Shanghai 200240, China

Received 7 December 2006; accepted 11 April 2007
Available online 20 July 2007

Abstract

A novel double heat pipe type adsorber, which uses compound adsorbent of $CaCl_2$ and expanded graphite to improve the adsorption performance, is designed. The double heat pipes are integrated into the adsorbers in order to solve the problem of the corrosion between seawater and the steel adsorber in ammonia system and improve the heat transfer performance of the adsorber. There are two kinds of heat pipes integrated with the adsorber. One is the split type heat pipe for heating the adsorber in desorption phase, the other one is the two-phase closed thermosyphon heat pipe for cooling the adsorber in adsorption phase. The performance of two-adsorber adsorption chiller integrated with double heat pipes is predicted. The heat transfer performance of the heat pipes can meet the heat demands for adsorption/desorption of the adsorbent when the heating/cooling time is 720 s and mass recovery time is 60 s. When the exhaust gas temperature is 550 °C, the cooling water temperature is 25 °C, the inlet and outlet chilled water is −10 and −15.6 °C, respectively; the simulation results show that the cooling power and COP of this adsorption system are 5.1 kW and 0.38, respectively.

Keywords: Adsorption refrigeration; Heat pipe; Exhausts gas; Calcium chloride; Expanded graphite; Ammonia

1. Introduction

Adsorption refrigerator and heat pump have been thought to be environmentally benign and cost-effective when driven by recovered waste heat [1]. In comparison with absorption systems, an adsorption system has no such problems as coolant pollution, crystallization and fractionation, while in comparison with vapor compression refrigerating systems, it has the advantages of simple control, low initial investment and less noise [2–4].

For an adsorption system that uses the refrigerant of ammonia, copper cannot be used to manufacture the adsorber for ammonia due to the corrosion of copper by the refrigerant. Moreover, the adsorber of an ammonia system cannot be cooled directly by water because of the possible corrosion between water and the material of adsorber, which is always steel. Such indirect heat transfer process will reduce the heat transfer performance. Furthermore, with the application of a medium heat transfer fluid between the hot or cold source and adsorber, the whole system will add much more valves to switch the medium heat transfer fluid between hot source and cold source. That will decrease the reliability and increase the cost of the system.

Heat pipes are reasonable for cooling and heating in adsorption refrigeration systems, not only due to its high heat flux density, but also due to the absence of any moving parts to drive the heat transfer medium. Vasiliev et al. have successfully demonstrated the use of heat pipes in adsorption refrigerators [5–7].

With good design ideas, it is possible to use heat pipes to heat or cool adsorbers, which put the adsorbers in contact with the heat-pipe working medium for heating and cooling [8]. Wang et al. [9] used the two-phase closed thermosyphon type heat pipe to heat and cool the adsorber, the heat transfer performance is simulated and the simulated results show that the average heating/cooling power for desorption/adsorption are 571/643 W, which could meet the heating/cooling demands of adsorbent for

*Corresponding author. Fax: +86 2134206776.
E-mail address: jywu@sjtu.edu.cn (J.Y. Wu).

0960-1481/$ - see front matter © 2007 Elsevier Ltd. All rights reserved.
doi:10.1016/j.renene.2007.04.023

Nomenclature

A	sectional area (m^2)
A_{k24}	constant Arrhenius factor from $CaCl_2 \cdot 2NH_3$ to $CaCl_2 \cdot 4NH_3$ (s^{-1})
A_{k48}	constant Arrhenius factor from $CaCl_2 \cdot 4NH_3$ to $CaCl_2 \cdot 8NH_3$ (s^{-1})
c_a	specific heat of adsorbent ($kJ\,kg^{-1}\,K^{-1}$)
c_{al}	specific heat of aluminum ($kJ\,kg^{-1}\,K^{-1}$)
c_{fe}	specific heat of steel ($kJ\,kg^{-1}\,K^{-1}$)
$c_{p,n}$, $c_{p,y}$	specific heat of gaseous ammonia and liquid ammonia ($kJ\,kg^{-1}\,K^{-1}$)
$c_{p,f}$	specific heat of exhaust gas ($kJ\,kg^{-1}\,K^{-1}$)
$c_{p,wl}$	specific heat of chilled fluid ($kJ\,kg^{-1}\,K^{-1}$)
COP	coefficient of performance
L	latent heat of ammonia ($kJ\,kg^{-1}$)
K_{eq}	constant value in the adsorption rate equation
$(KA)_{ad}$	heat transfer coefficient of adsorber in adsorption phase ($kW\,K^{-1}$)
$(KA)_c$	heat transfer coefficient of condenser ($kW\,K^{-1}$)
$(KA)_{de}$	heat transfer coefficient of adsorber in desorption phase ($kW\,K^{-1}$)
$(KA)_e$	heat transfer coefficient of evaporator ($kW\,K^{-1}$)
$\dot{m}_{cool}$	Mass flow rate of chilling water ($kg\,s^{-1}$)
$\dot{m}_{cool}$	mass flow rate of cooling water ($kg\,s^{-1}$)
$\dot{m}_{e,de}$	mass flow rate of refrigerant evaporated in the evaporator corresponding to the desorbing chamber in the mass recovery process ($kg\,s^{-1}$)
$\dot{m}_{e,cond}$	mass flow rate of refrigerant corresponding to condensed in the evaporator corresponding to the adsorbing chamber in the mass recovery process ($kg\,s^{-1}$)
$\dot{m}_f$	mass flow rate of exhaust gas ($kg\,s^{-1}$)
$\dot{m}_{mr}$	mass flow rate of refrigerant in the mass recovery process ($kg\,s^{-1}$)
m_{24}, m_{48}	kinetics parameters of adsorption rate equation
M_a	mass of adsorbent (kg)
M_c	mass of ammonia condenser (kg)
M_e	mass of evaporator (kg)
$M_{e,0}$	mass of liquid refrigerant at the equilibrium state (kg)
$M_{e,w}$	mass of ammonia in the evaporator (kg)
$M_{fin,ad}$	mass of aluminum fins (kg)
$M_{t,ad}$	mass of heat transfer tube (kg)
n_{24}, n_{48}	kinetics parameters of adsorption rate equation
P_{eq}	equilibrium pressure (Pa)
$P_{n,des}$	the pressure of evaporator corresponding to the adsorber in desorption phase (Pa)
$P_{n,ads}$	the pressure of evaporator corresponding to the adsorber in adsorption phase (Pa)
q_{st}	adsorption heat (kJ kg)
Q_{ref}	cooling power of the system (kW)
Q_h	heating power of the system (kW)
T	temperature (K)
T_a	temperature of adsorber (K)
$T_{ad,in}$	cooling water inlet temperature of condenser corresponding to cooling heat pipe (K)
$T_{ad,out}$	cooling water outlet temperature of condenser corresponding to cooling heat pipe (K)
T_c	condenser temperature (K)
$T_{chill,in}$	chilled fluid inlet temperature (K)
$T_{chill,out}$	chilled fluid outlet temperature (K)
$T_{cool,in}$	cooling water inlet temperature of condenser (K)
$T_{cool,out}$	cooling water outlet temperature of condenser (K)
T_e	evaporator temperature (K)
T_{eq}	equilibrium temperature (K)
$T_{f,in}$	exhaust gas inlet temperature of exhaust gas-water heat exchanger (K)
$T_{f,out}$	exhaust gas inlet temperature of exhaust gas-water heat exchanger (K)
t	time (s)
v_{nv}	specific volume of gaseous ammonia ($m^3\,kg^{-1}$)
X	the global conversation of adsorbent from $CaCl_2 \cdot 2NH_3$ to $CaCl_2 \cdot 8NH_3$, $X = x/x_{max,}$
X_{24}	the global conversation of adsorbent from $CaCl_2 \cdot 2NH_3$ to $CaCl_2 \cdot 4NH_3$
X_{48}	the global conversation of adsorbent from $CaCl_2 \cdot 4NH_3$ to $CaCl_2 \cdot 8NH_3$
x_{max}	the maximum adsorption capacity of adsorbent ($kg\,kg^{-1}$)

Greek letters

ΔH	enthalpy of transformation for Clausius–Clapeyron equation ($J\,mol^{-1}$)
ΔS	entropy of transformation for Clausius–Clapeyron equation ($J\,mol^{-1}\,K^{-1}$)
ε	porosity of the adsorbent
$\Delta_{1,2,3}$	process index
τ	time function (s)
ρ_{SB}	molar density of salt in the compound adsorbent ($mol\,m^{-3}$)

Subscripts

24	related to the reaction to convert $CaCl_2 \cdot 2NH_3$ to $CaCl_2 \cdot 4NH_3$
48	related to the reaction to convert $CaCl_2 \cdot 4NH_3$ to $CaCl_2 \cdot 8NH_3$
EG	expanded graphite
eq	equilibrium state
ads	adsorption phase
des	desorption phase
in	inlet
out	outlet

adsorption/desorption, respectively in a cycle time of 10 min. In the base of this research, Wang et al. integrated the split type heat pipe into the adsorber to heat and cool adsorber and built a chemical adsorption refrigeration test rig [10–12]. The experimental results show that at the evaporating temperature of –15 °C, its average cooling power is 1.37 kW, refrigeration COP is 0.41 and SCP is 731 W kg^{-1} for each adsorber.

Wang et al. [13,14] combined a heat-pipe heat exchanger with the evaporators of two adsorption/desorption units to output continuous refrigerating capacity in a novel silica gel–water adsorption chiller. Yang et al. [15] also combined a gravity heat pipe into the silica gel–water adsorption room air conditioner.

For solving the problem of corrosion between seawater and the steel adsorber in ammonia system, improving the heat transfer performance of the adsorber and decreasing the number of valves used in the system, a novel double heat pipe type adsorber is designed and simulated. The heating pipe of the split type to heat the adsorber; the cooling pipe is the two-phase closed thermosyphon type heat pipe to cool the adsorber. The results show that this novel type adsorber can work in a highly effective way, and the heat and mass transfer of the adsorber satisfy the requirements.

2. System description

Fig. 1 shows the structure of the designed double heat pipe type adsorption chiller. This novel adsorption chiller is composed of two working parts, including Part I and Part II. Part I is the ammonia thermal compressor, Part II is the ammonia refrigerator. Part I is composed of three components: condensers, adsorbers and exhaust gas–water heat exchanger. The condensers (20 in Fig. 1) are shell-tube heat exchanger, which the cooling water flows inside the tubes and the cooling heat pipe working medium (water vapor) condenses on the outside surface of tubes. The function of condensers is to condensate the working medium (water vapor) in the cooling heat pipe and takes out of heat in the adsorber. Expanded graphite (EG)–$CaCl_2$ compound adsorbent (10 in Fig. 1) is filled in the adsorber. There are two adsorbers (2 in Fig. 1) in part I, so the ammonia could be adsorbed in or desorbed out of the adsorbers from the ammonia refrigerator alternately. The exhaust gas–water heat exchanger (6 in Fig. 1) is also a shell-tube heat exchanger, in which the exhaust gas flows through the tubes and the water is heated and evaporated on the outside surface of tubes. The function of exhaust gas–water heat exchanger is to obtain heat from the exhaust gas and supply it to the adsorber.

Part II is composed of two components, namely ammonia condensers (16 in Fig. 1) and ammonia flooded evaporators (17 in Fig. 1). The function of ammonia condensers is to condensate desorbed ammonia from adsorber in desorption phase. The adsorber would adsorb ammonia in the evaporator in adsorption phase and the evaporation of ammonia inside evaporator provides refrigeration effect to chilled fluid.

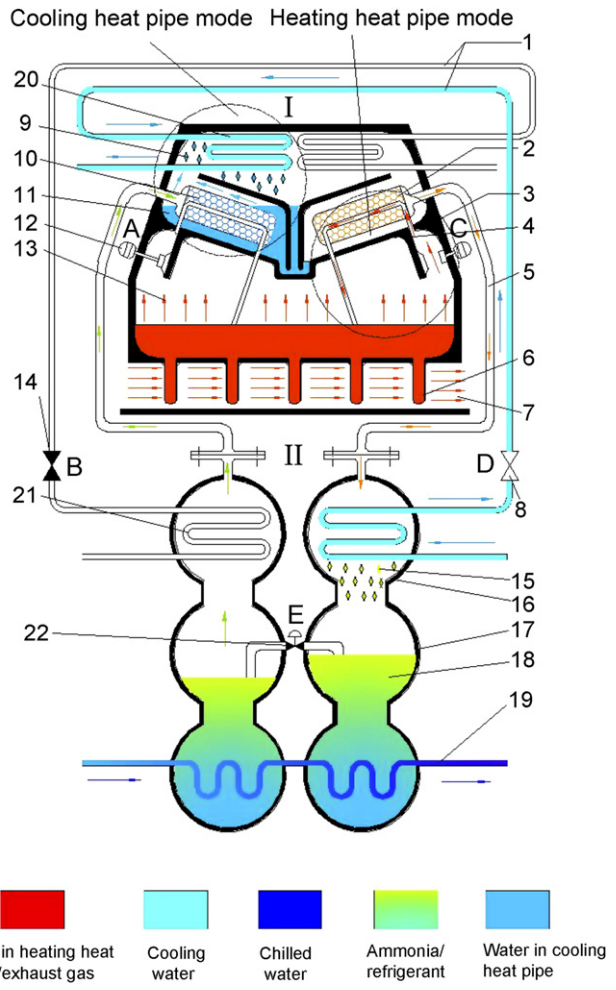

Fig. 1. Schematic diagram of the designed double heat pipe type adsorption chiller: I. ammonia thermal compressor; II. ammonia refrigerator; 1. cooling water cycle; 2. adsorber; 3. shell of the ammonia thermal compressor; 4. water vapor channel of heating heat pipe; 5. ammonia channel; 6. exhaust gas-water heat exchanger; 7. exhaust gas; 8. ball valve for cooling water; 9. condensed water in cooling heat pipe; 10. compound adsorbent; 11. cooling heat pipe working medium (water); 12. butterfly valve for water vapor; 13. heating heat pipe working medium (water vapor); 14. ball valve for cooling water; 15. condensed ammonia; 16. ammonia condenser; 17. flooded ammonia evaporator; 18. liquid ammonia; 19. chilled water cycle; 20. condenser for cooling heat pipe; 21. condenser for ammonia vapor; 22. ball valve for mass recovery between two evaporators.

There are two ammonia condensers and two ammonia flooded evaporators. One ammonia condenser and one ammonia flooded evaporator are composed of an independent ammonia refrigerator unit, which is connected to adsorber in the part I. Two independent refrigerator units are linked by the mass recovery tube, the mass recovery ball valve (22 in Fig. 1) controls the open and close mass recovery tube. Both the ammonia condensers and ammonia flooded evaporators are shell-tube heat exchangers, cooling water and chilled water flow into the tube and ammonia is condensed or evaporated on the outside of the tube.

There are only five valves for one whole system. Valves A and C control the water vapor coming into the adsorber, valves B and D control the cooling water flowing into the condensers. Valve E controls the mass recover open or close between one two ammonia evaporators.

2.1. Cooling heat pipe

The cooling heat pipe is of two-phase closed thermosyphon type. As shown in Fig. 1, the cooling heat pipe is composed of two parts, evaporation zone and condensation zone. The evaporation zone is the outside surface of the adsorber and the condensation zone is the condenser. The working medium of cooling heat pipe is water.

Fig. 1 shows valve D is opened and valve B is closed. When the cooling heat pipe working medium flows into the evaporation zone, it is heated and evaporated to be water vapor (because the temperature of adsorber is very high after desorption process). In the phase change process from water to water vapor, the heat of adsorber is transferred efficiently to working medium of cooling heat pipe (the latent heat of vaporization of water is 2258 kJ kg^{-1}). So the adsorber temperature decreases quickly during the vaporization process. The water vapor condenses on the condensation zone when the cooling water flows through the condenser. In this phase change process from water vapor to water, the heat of water vapor is transferred efficiently to the cooling water. The condensed water (9 in Fig. 1) falls back to the evaporation zone and it would be evaporated again. In this process, the adsorbent temperature decreases and ammonia is adsorbed by the adsorbent.

2.2. Heating heat pipe

The heating heat pipe is of split type. As shown in Fig. 1, the heating heat pipe is also composed of two parts, evaporation zone and condensation zone. The evaporation zone is the exhaust gas–water heat exchanger and the condensation zone is the heating heat pipe channel inside the adsorber. The working medium of heating heat pipe is water.

Fig. 1 shows valve C is opened and valve A is closed. Water is heated to water vapor by exhaust gas in the exhaust gas-water exchanger. Then the water vapor comes to the adsorber and condenses on the surface of heating heat pipe channel (4 in Fig. 1) inside the adsorber. In the phase change process from water vapor to water, the heat of water vapor is transferred efficiently to the adsorber. So the adsorber temperature increases quickly during the condensation process. The condensed water flows back to the evaporation zone through heating heat pipe channel. In this process, the adsorbent temperature increases and ammonia is desorbed out of the adsorbent.

2.3. Compound adsorbent

The compound adsorbent is a mixture of $CaCl_2$ and EG and the refrigerant is NH_3. This compound adsorbent has been studied for its adsorption performance and heat transfer performance in our previous works [16–18]. In these researches, the addition of EG in $CaCl_2$ solved the agglomeration problem that happened in the repeated adsorption/desorption reaction of $CaCl_2$ and NH_3 and improved the adsorption capacity of $CaCl_2$. Also the consolidated compound adsorbents of $CaCl_2$ and EG have higher thermal conductivity than that of $CaCl_2$ powder.

2.4. Working principle

The cycle process of the designed double heat pipe type adsorption chiller is different from that of the conventional two-bed single-stage adsorption chiller. As an example, the chiller startup is from the adsorption phase for the left adsorber and desorption phase for the right adsorber (as shown in Fig. 1). The whole cycle process has four modes:

(1) *Left adsorber in adsorption phase and right adsorber in desorption phase*: As shown in Fig. 1, in this process valve C and valve D are opened and valve A, valve B and valve E are closed. At the moment of start, temperature of left adsorber is high (about 120 °C) because it just finished desorption phase, temperature of right adsorber is low (about 40 °C) because it just finished adsorption phase. When valve C is opened, water vapor flows into the right adsorber to heat the adsorber. Thus, the heating heat pipe in right adsorber starts to work and the temperature of right adsorber increases. The refrigerant vapor desorbed from the right adsorber is cooled down to condenser temperature in the ammonia condenser by the cooling water. Then it falls down to the right evaporator. In desorption process of right adsorber, the pressure in the right chamber also increases with temperature. When the pressure in right chamber is higher than in left chamber, the working medium of cooling heat pipe in right chamber is pushed to the left chamber. When valve D is opened, the cooling heat pipe starts to work and the temperature of left adsorber decreases. The left adsorber is in adsorption phase. The refrigerant (NH_3) in left evaporator is evaporated at the evaporating temperature and seizes heat from the chilled water. The compound adsorbed in the left adsorber adsorbs the evaporated refrigerant vapor and the adsorption heat is transferred to the cooling water by the cooling heat pipe. At the end of this mode, there is ammonia liquid level difference between the left and right evaporators. So the next mode is the mass recovery process between the left and right ammonia flooded evaporators.

(2) *Mass recovery from right ammonia flooded evaporator to left ammonia flooded evaporator*: As shown in Fig. 2(a), in this mode valve E is opened. When the adsorption and desorption process is over, the quantity and pressure of ammonia in left and right flooded evaporators are different (level of ammonia in right evaporator is higher than in left evaporator). For keeping the same quantity of ammonia in one left and right evaporators, valve E is opened. Because of the huge pressure difference between the left and right evaporators, ammonia in the right evaporator flows into

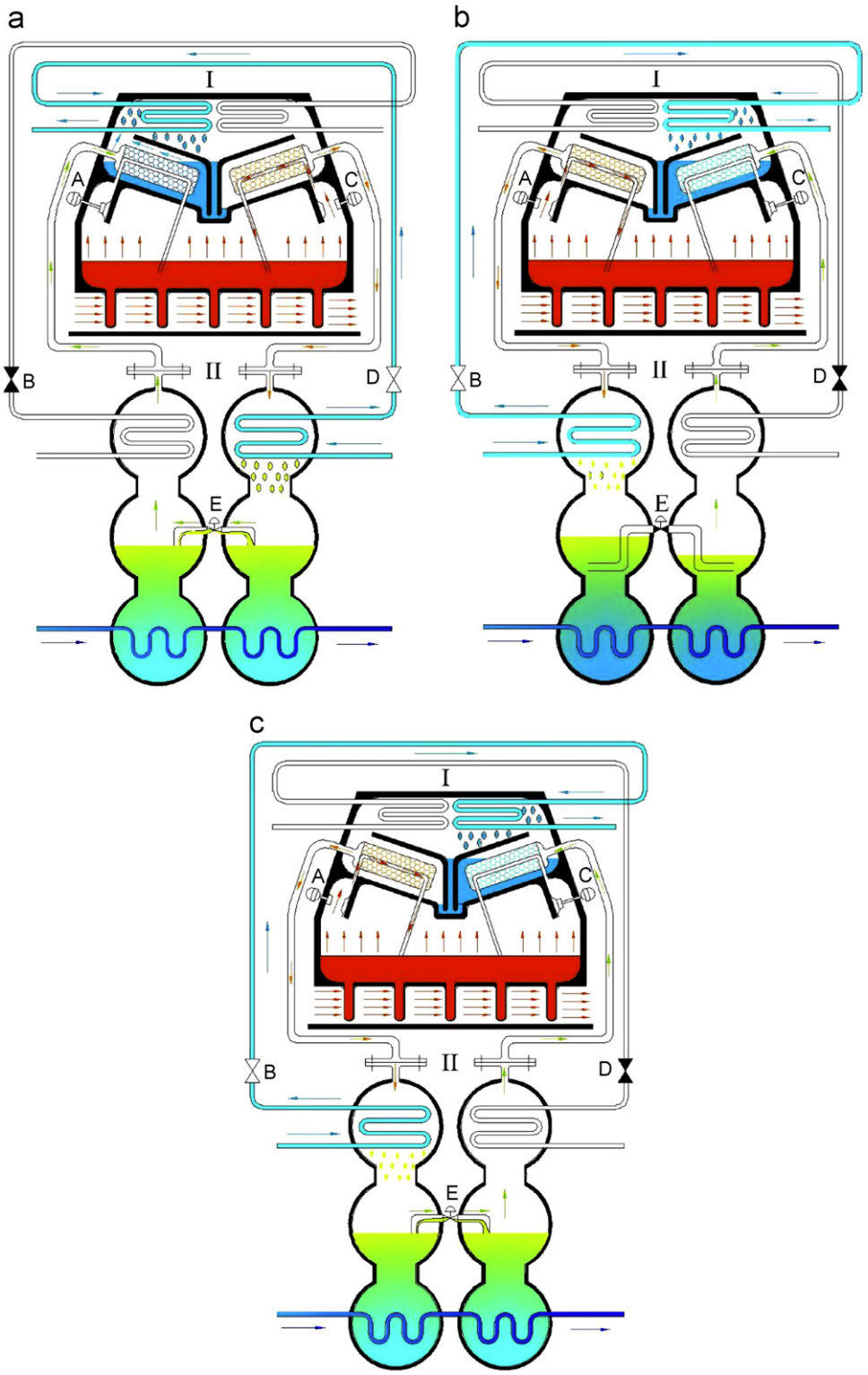

Fig. 2. (a) Mass recovery process (from right evaporator to left evaporator); (b) left adsorber in desorption phase and right adsorber in adsorption phase and (c) mass recovery process (from left evaporator to right evaporator).

the left evaporator in a very short time. When the ammonia pressure in the two evaporators reaches equilibrium, the mass recovery mode finishes and valve E is closed.

(3) *Left adsorber is in desorption phase and right adsorber is in adsorption phase*: As shown in Fig. 2(b), in this mode valve A and valve B are opened and valve C, valve D and valve E are closed. The working principle in this mode is almost the same as in mode (1). In this process, the left adsorber is in desorption phase and the right adsorber is in adsorption phase. At the end of this mode, there is

ammonia liquid level difference between the left and right evaporators.

(4) *Mass recovery from left flooded evaporator to right ammonia flooded evaporator*: As shown in Fig. 2(c), in this mode valve E is opened. The working principle in this mode is almost the same as in mode (2). When valve E is opened, ammonia will flow from left evaporator into the right evaporator. While the ammonia pressure in the two evaporators reaches equilibrium, the mass recovery mode finishes and valve E is closed.

3. Mathematical model

In this simulation, a mathematical model based on lumped parameters is introduced. In order to simplify the analysis, some assumptions are generally made as follows:

(1) Since the fin-tube adsorber has high heat transfer efficiency, the temperature of the adsorbent is uniform;
(2) The pressure of ammonia in the adsorber is uniform because the mass transfer channel is quite large inside the adsorber;
(3) The refrigerant is adsorbed uniformly in the adsorber and it is gaseous in the adsorbent;
(4) The evaporating temperature is identical to the temperature of the liquid in the evaporator;
(5) The heat conduction of the shell connecting the adsorber to the condenser or the evaporator is neglected;
(6) The system has no heat losses (or refrigerating output loss) to the environment.

3.1. Adsorption equations

A nonequilibrium adsorption/desorption process occurs in a practical adsorption cooling system with reactions (1) and (2). So a nonequilibrium adsorption rate equation is used in the simulation [19]:

$$CaCl_2 \cdot 8NH_3 + \Delta H_1 \overset{P_1,T_1}{\longleftrightarrow} CaCl_2 \cdot 4NH_3 + 4NH_3, \tag{1}$$

$$CaCl_2 \cdot 4NH_3 + \Delta H_2 \overset{P_2,T_2}{\longleftrightarrow} CaCl_2 \cdot 2NH_3 + 2NH_3, \tag{2}$$

$$\frac{dX_{24}}{dt} = A_{k24}(1-X_{24})^{n_{24}}\left(\frac{P\varepsilon}{RT\rho_{SB}}\right)^{m_{24}} K_{eq24} \times \ln\left(\frac{P}{P_{eq24}}\right)\left(\frac{1}{T}-\frac{1}{T_{eq24}}\right), \tag{3}$$

$$\frac{dX_{48}}{dt} = A_{k48}(X_{24}-X_{48})^{n_{48}}\left(\frac{P\varepsilon}{RT\rho_{SB}}\right)^{m_{48}} K_{eq48} \times \ln\left(\frac{P}{P_{eq48}}\right)\left(\frac{1}{T}-\frac{1}{T_{eq48}}\right), \tag{4}$$

where X is the global conversation of adsorbent, $X = x/x_{max}$; T is the temperature of adsorbent, P the pressure of the adsorbent, ε the porosity of the adsorbent, ρ_{SB} the molar density of salt in the compound adsorbent, A_k the constant Arrhenius factor and the value of K_{eq} is 0.5. P_{eq} and T_{eq} were calculated by the Clausius–Clapeyron equation

$$\ln(P_{eq}) = -\frac{\Delta H}{RT} + \frac{\Delta S}{R}. \tag{5}$$

The global conversion of adsorbent in the adsorber was calculated by considering the contribution of each reaction in the total adsorbed ammonia as follows:

$$\frac{dX}{dt} = \frac{(4(dX_{48}/dt) + 2(dX_{24}/dt))}{6}. \tag{6}$$

The parameters of Eqs. (3) and (4) are identified by the experimental data tested by Olivera [19], and the value of these parameters is listed in Table 1.

3.2. Energy equations

(1) *Energy balance for adsorber*: The heating and cooling heat pipes are taken as one part in the desorber and adsorber, and the function of heat pipes are taken into account by the heat transfer coefficient of adsorber $(KA)_{ad}$ and heat transfer coefficient of desorber $(KA)_{de}$.

$$\begin{aligned}\frac{d}{d\tau}\{[M_a(c_a + c_{p,n}Xx_{max}) + c_{fe}M_{t,ad} + c_{al}M_{fin,ad}]T_a\} &= M_a q_{st}\frac{dX}{d\tau}x_{max} + (1-\delta_1)c_{n,v}M_a\frac{dX}{d\tau}x_{max}(T_e - T_a) \\ &\quad + (1-\delta_1)\dot{m}_{cool}c_{p,w}(T_{ad,in} - T_{ad,out}) \\ &\quad + \delta_1\dot{m}_f c_{p,f}(T_{f,in} - T_{f,out}),\end{aligned} \tag{7}$$

where δ_1 is the process index:

$$\delta_1 = \begin{cases} 1, & \text{desorption process} \\ 0, & \text{adsorption process} \end{cases}, \tag{8}$$

$$\delta_1 = \begin{cases} 1, & \frac{T_{f,out}-T_a}{T_{f,in}-T_a} = \exp\left[\frac{-(KA)_{de}}{\dot{m}_f c_{p,f}}\right] \\ 0, & \frac{T_{w,out}-T_a}{T_{w,in}-T_a} = \exp\left[\frac{-(KA)_{ad}}{\dot{m}_{cool}c_{p,w}}\right] \end{cases}. \tag{9}$$

(2) *Energy balance for condenser*:

$$c_{fe}M_c\frac{dT_c}{d\tau} = \delta_1\left[LM_a\frac{dX_{des}}{d\tau}x_{max} + c_{nv}M_a\frac{dX_{des}}{d\tau}x_{max}(T_c - T_a) + \dot{m}_{cool}c_{p,w}(T_{cool,in} - T_{cool,out})\right], \tag{10}$$

$$\frac{T_{cool,out} - T_c}{T_{cool.in} - T_c} = \exp\left[\frac{-(KA)_c}{\dot{m}_{cool}c_{p,w}}\right]. \tag{11}$$

Table 1
Identified kinetics parameter of adsorption rate equation

A_{k24} (s^{-1})	n_{24}	m_{24}	A_{k48} (s^{-1})	n_{48}	m_{48}
2.24×10^5	2	2	2.05×10^4	1	1

(3) *Evaporator*:

$$\frac{\mathrm{d}}{\mathrm{d}\tau}[(c_{\mathrm{p,w}}M_{\mathrm{e,w}}+c_{\mathrm{fe}}M_{\mathrm{e}})T_{\mathrm{e}}] = (1-\delta_1)[-LM_{\mathrm{a}}\frac{\mathrm{d}X_{\mathrm{ads}}}{\mathrm{d}\tau}x_{\max}+\dot{m}_{\mathrm{chill}}c_{\mathrm{pwl}}(T_{\mathrm{chill,in}}-T_{\mathrm{chill,out}})] + \delta_1[c_{\mathrm{p,n}}(T_{\mathrm{e}}-T_{\mathrm{c}})M_{\mathrm{a}}\frac{\mathrm{d}X_{\mathrm{des}}}{\mathrm{d}\tau}x_{\max}], \quad (12)$$

$$\frac{T_{\mathrm{chill,out}}-T_{\mathrm{e}}}{T_{\mathrm{chill,in}}-T_{\mathrm{e}}} = \exp\left[\frac{-(\mathrm{KA})_{\mathrm{e}}}{\dot{m}_{\mathrm{chill}}c_{\mathrm{p,w}}}\right]. \quad (13)$$

3.3. Liquid refrigerant equilibrium in evaporator

$$\frac{\mathrm{d}M_{\mathrm{e,w}}}{\mathrm{d}\tau} = M_{\mathrm{e,0}} - M_{\mathrm{a}}\frac{\mathrm{d}X_{\mathrm{ads}}}{\mathrm{d}\tau}x_{\max}, \quad (14)$$

where $M_{\mathrm{e,0}}$ is the mass of liquid refrigerant at the equilibrium state.

3.4. Equilibrium equations in the mass recovery process

When the adsorption and desorption process is over, the quantity and pressure of ammonia in left and right flooded evaporators are different. For keeping the same quantity of ammonia in the left and right evaporators, the mass recovery valve is opened. Because of huge pressure difference between the left and right evaporators, the ammonia in one evaporator flows into another evaporator in a very short time. When the ammonia pressure in the two evaporators reaches equilibrium, the mass recovery mode finishes.

Energy balance of evaporator:

$$\frac{\mathrm{d}}{\mathrm{d}\tau}[(c_{\mathrm{p,v}}M_{\mathrm{e,v}}+c_{\mathrm{fe}}M_{\mathrm{e}})T_{\mathrm{e}}] = -L\delta_2+\delta_3\dot{m}_{\mathrm{chill}}c_{\mathrm{p,wl}}(T_{\mathrm{chill,in}}-T_{\mathrm{chill,out}})], \quad (15)$$

where

$$\delta_2 = \begin{cases} \dot{m}_{\mathrm{e,evap}} & \text{for desorbing chamber} \\ \dot{m}_{\mathrm{e,cond}} & \text{for adsorbing chamber} \end{cases}, \quad (16)$$

$$\delta_3 = \begin{cases} 1, & T_{\mathrm{e}} \leqslant T_{\mathrm{chill,in}} \\ 0, & T_{\mathrm{e}} > T_{\mathrm{chill,in}} \end{cases}, \quad (17)$$

where $\dot{m}_{\mathrm{e,evap}}$ and $\dot{m}_{\mathrm{e,cond}}$ are, respectively, the mass flow rates of refrigerant evaporated in the evaporator corresponding to the desorbing chamber and condensed in the evaporator corresponding to the adsorbing chamber.

Mass equilibrium:

$$M_{\mathrm{a}}\frac{\mathrm{d}X_{\mathrm{des}}}{\mathrm{d}\tau}x_{\max}+\dot{m}_{\mathrm{e,evap}} = \dot{m}_{\mathrm{e,cond}} - M_{\mathrm{a}}\frac{\mathrm{d}X_{\mathrm{ads}}}{\mathrm{d}\tau}x_{\max} = \dot{m}_{\mathrm{mr}}, \quad (18)$$

where $\dot{m}_{\mathrm{mr}}$ is the refrigerant mass flow rate in the mass recovery process.

The vapor is assumed as an incompressible flow and the flow resistance of ammonia vapor is neglected. The pressure drop between the two evaporators in the mass recovery process can be calculated as follows:

$$P_{\mathrm{n,des}} - P_{\mathrm{n,ads}} = \frac{v_{\mathrm{nv}}\dot{m}_{\mathrm{mr}}^2}{2A^2} \quad (19)$$

where A is the sectional area of mass recovery channel.

The Martin–Hou equation [20] is introduced to calculate the state parameters for ammonia vapor:

$$P_{\mathrm{n,v}} = \sum_{i=1}^{5}\frac{f_i(T)}{(V-b)^i} = \frac{RT}{V-b}+\frac{A_2+B_2T+C_2\exp(-KT/T_{\mathrm{c}})}{(V-b)^2} + \frac{A_3+B_3T+C_3\exp(-KT/T_{\mathrm{c}})}{(V-b)^3}+\frac{A_4}{(V-b)^4} + \frac{A_5+B_5T+C_5\exp(-KT/T_{\mathrm{c}})}{(V-b)^5}. \quad (20)$$

The values of parameters in the Martin–Hou equation for ammonia are listed in Ref. [20].

3.5. Performance parameters equations

Cooling power:

$$Q_{\mathrm{ref}} = \frac{\int_0^{\tau_{\mathrm{cycle}}} c_{\mathrm{p,wl}}\dot{m}_{\mathrm{chill}}(T_{\mathrm{chill,in}}-T_{\mathrm{chill,out}})\,\mathrm{d}\tau}{\tau_{\mathrm{cycle}}}, \quad (21)$$

Heating power:

$$Q_{\mathrm{h}} = \frac{\int_0^{\tau_{\mathrm{cycle}}} c_{\mathrm{p,f}}\dot{m}_{\mathrm{f}}(T_{\mathrm{h,in}}-T_{\mathrm{h,out}})\,\mathrm{d}\tau}{\tau_{\mathrm{cycle}}}, \quad (22)$$

$$\mathrm{COP} = \frac{Q_{\mathrm{ref}}}{Q_{\mathrm{h}}}. \quad (23)$$

4. Simulation procedure and experimental validity

The system of differential equations (Eqs. (3)–(20)) were solved simultaneously by numerical integration using finite-difference substitution in the derivatives. The temperature is assumed to be uniform in adsorbers, evaporators and condensers. For the specific heats of metals, adsorbent and adsorbate, average values are adopted throughout the entire temperature range. Refrigerant mass flows between evaporator and adsorber, condenser and desorber, adsorber and desorber are taken as equivalent in the model. The parameters considered in the simulation are shown in Table 2.

In the numerical solution of the equations, successive substitution of newly calculated values was used with six iterative nested loops in repeating the calculations until the discrepancy in heat balances was less than 2%; the converging factor is taken as 10^{-3} (or 0.001) for all

Table 2
Physical property parameters used in the simulation

Symbol	Value	Unit
$c_{p,w}$	4.180	kJ kg^{-1} K^{-1}
c_a	0.919	kJ kg^{-1} K^{-1}
c_{al}	0.905	kJ kg^{-1} K^{-1}
c_{fe}	0.465	kJ kg^{-1} K^{-1}
c_{nv}	3.180	kJ kg^{-1} K^{-1}
$c_{p,f}$	1.097	kJ kg^{-1} K^{-1}
$c_{p,wl}$	3.044	kJ kg^{-1} K^{-1}
q_{st}	2450	kJ kg^{-1}
KA_{de}	1123	W K^{-1}
KA_{ad}	1258	W K^{-1}
KA_c	1764	W K^{-1}
KA_e	11400	W K^{-1}
L	1330	kJ kg^{-1}
m_{chill}	0.31	kg s^{-1}
M_a	20.0	kg
$M_{fin,ad}$	22.0	kg
$M_{t,ad}$	88.0	kg
M_c	13	kg
M_e	29.4	kg
$M_{e,0}$	30	kg
x_{max}	0.8	kg/kg

parameters. The calculations are made with a time interval of 1 s.

5. Result and discussion

5.1. Heating/cooling time

Fig. 3 shows the cooling power and COP variation with heating/cooling time. The COP increases a little with the extension of the heating/cooling time when the exhaust gas temperature is 550 and 350 °C. The cooling power decreases with longer heating/cooling time. There is a cross point between the COP curve and cooling power curve in Fig. 7 when the heating/cooling time is 720 s and the exhaust temperature is 550 °C. Thus the optimal heating/cooling time for this system is 720 s when the exhaust gas temperature is 550 °C. The COP and cooling power are 0.38 and 5.1 kW, respectively, when the heating/cooling time is 720 s and exhaust gas temperature is 550 °C. The COP and cooling power are 0.31 and 4.2 kW, respectively, when the heating/cooling time is 630 s and the exhaust gas temperature is 350 °C. The mass of adsorbent is 20 kg in each adsorber.

Fig. 4 shows the mass recovery time variation with COP of the adsorption system. In the range of mass recovery time 0–250 s, the COP gets its maximum value when the mass recovery time is 60 s and the exhaust gas is 550 or 350 °C. The reason for the variation of COP is that there is a huge pressure drop (about 2.5 MPa) between the two evaporators when the mass recovery happens. The mass recovery process will finish in a very short time and there is no sense in extending the recovery time to increase the cooling power output. So the value of COP will decrease

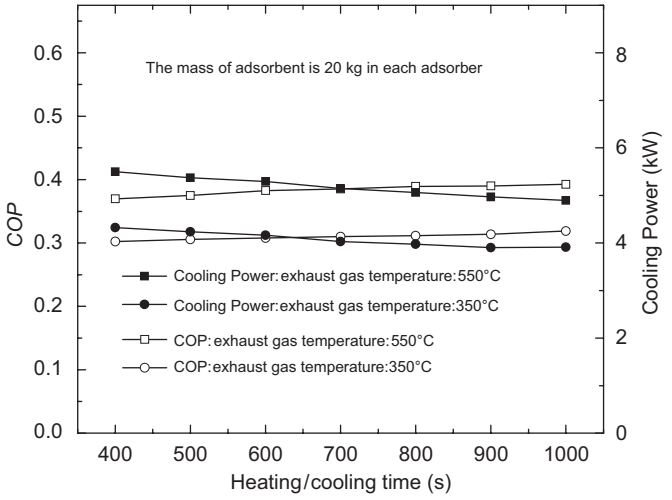

Fig. 3. Variation of the heating/cooling time with the cooling power and COP (60 s mass recovery time, cooling water inlet temperature: 25 °C, chilling fluid inlet temperature: −10 °C).

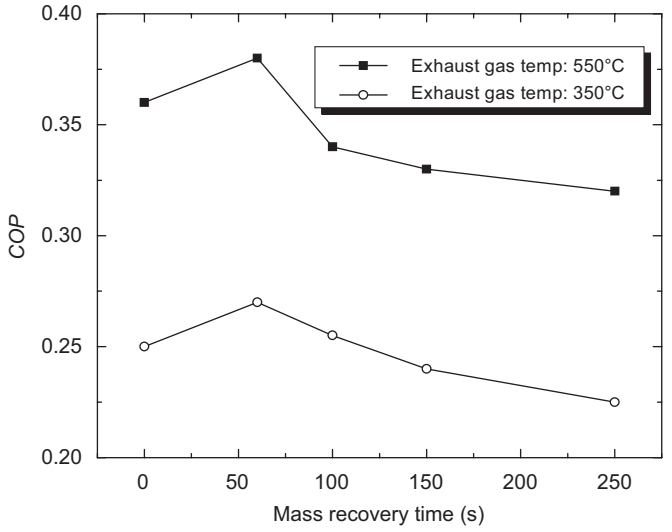

Fig. 4. Variation of the mass recovery time on the COP (720 s heating/cooling time).

when the mass recovery time is longer than the optimal value (60 s).

5.2. Heat transfer fluid temperature variation

Fig. 5 shows the temperature profile of the cooling water when the heating/cooling time is 720 s and the mass recovery time is 60 s. The inlet temperature of cooling water is 25 °C. As shown in Fig. 1, the cooling water flows into the right ammonia condenser to condensate ammonia and then comes into the left condenser to condensate the cooling heat pipe working medium (water). It is shown in Fig. 5 that the cooling water outlet temperature increases from 25 to 43 °C in 0s to 200 s. This indicates that the heat released by ammonia and water is higher than what the

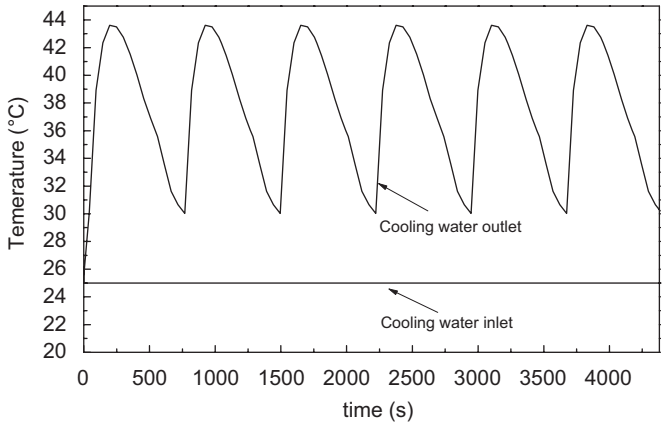

Fig. 5. Temperature profile of cooling water (720 s heating/cooling time, 60 s mass recovery time, cooling water inlet temperature: 25 °C, chilling fluid inlet temperature: −10 °C).

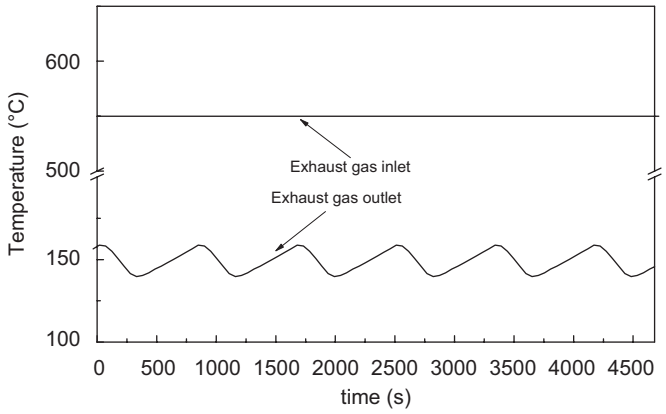

Fig. 6. Temperature profile of exhaust gas (720 s heating/cooling time, 60 s mass recovery time, cooling water inlet temperature: 25 °C, chilling fluid inlet temperature: −10 °C).

cooling water could transport and the temperature of cooling water increases in the beginning. Later the heat released by ammonia and water become smaller from 200 to 780 s so that the cooling water temperature decreases from 43 to 30 °C.

Fig. 6 shows the temperature profile of exhaust gas. As shown in Fig. 6, the exhaust gas outlet temperature changed from 165 to 145 °C when the two adsorbers switched (valve B and valve D switched). The reason for this is the different heat consumption of adsorbers in the desorption process. Before the valves switched, the adsorber is at the end of desorption process and the thermal energy it needed is small. After the valves switched, the adsorber is at the beginning of desorption process and the thermal energy needed is quite large. So the variation trend of exhaust gas outlet temperature is a gradual increase and then a gradual decrease when the valves switched.

Fig. 7 shows the variation of chilled fluid temperature. Chilled fluid outlet temperature reduces to −14.8 °C in the adsorption process. Then it decreases sharply to the lowest

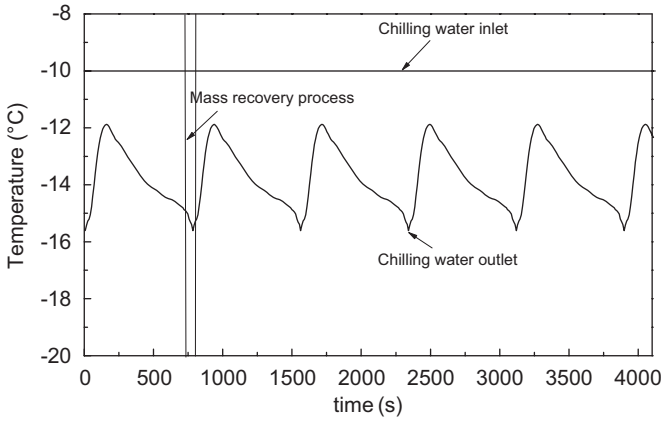

Fig. 7. Temperature profile of chilled fluid (720 s heating/cooling time, 60 s mass recovery time, cooling water inlet temperature: 25 °C, chilled fluid inlet temperature: −10 °C).

temperature, about −15.6 °C, because of the mass recovery process that happens between the two evaporators. At the end of the mass recovery process, there is no more cooling power output from the evaporators so the chilled fluid temperature would increase to the highest temperature again.

5.3. Adsorber temperature variation

Fig. 8 shows the variation of adsorber temperature. The speeds of adsorber temperature variation in desorption/adsorption phase are the evaluation criteria of the adsorber heat transfer performance. For right adsorber, when the right adsorber switches from adsorption phase to desorption phase, the temperature increases from 43 to 118 °C in 12 min. Then the right adsorber starts adsorption process and the temperature decreases from 118 to 43 °C in 12 min. The cycle time is 24 min and the temperature variation range is 118–43 °C. In comparison with the test results of split heat pipe type adsorption test rig [21], the adsorber temperature variation range is 100–35 °C and the cycle time is 50 min, the heat pipe working media is water. Obviously, the heat transfer performance of double heat pipe adsorber is better than that of the split heat pipe type adsorber. It costs only half-cycle time of split heat pipe type adsorber and the temperature variation range is even larger than in split heat pipe type adsorber.

Fig. 8 also shows the influence of mass recovery that happens in ammonia evaporator at the adsorber temperature. When the mass recovery happens at the end of desorption phase, the adsorber temperature decreases first and then increases. When the mass recovery happens at the end of adsorption phase, the adsorber temperature decreases first and then increases. At the beginning of mass recovery process, the right adsorber desorbs a lot of refrigerant in a very short time because of the huge pressure difference between the two adsorbers. The desorption reaction is endothermic, the heat that the right adsorber

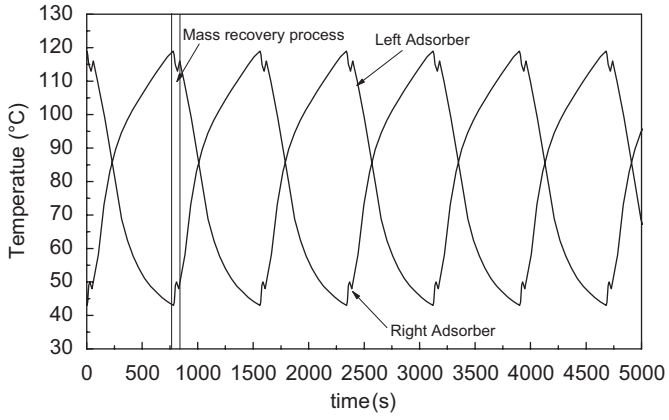

Fig. 8. Temperature profile of adsorber (720 s heating/cooling time, 60 s mass recovery time, cooling water inlet temperature: 25 °C, chilled fluid inlet temperature: −10 °C).

needs exceeds the supplement of heating heat pipe so the adsorber temperature decreases first. With the proceeding of mass recovery process, the desorption reaction become slow and the heat given by the heating heat pipe exceeds that adsorber needed by the and the temperature of right adsorber increases consequently. For the mass recovery process of left adsorber, the adsorption reaction is an exothermal reaction. So the adsorber temperature variation is reverse trend with the mass recovery process of right adsorber.

6. Conclusions

A novel chemical adsorption chiller integrated with double heat pipes for heating and cooling the adsorber is designed and simulated. This system employs the $CaCl_2$/EG–ammonia as working pair and is driven by the waste heat of exhaust gas. There are two types heat pipe integrated with the adsorber. One is the split type heat pipe for heating the adsorber in desorption phase, the other is the two-phase closed thermosyphon for cooling the adsorber in adsorption phase. As the simulation using the lumped parameters model shows, the cooling power is more than 5 kW and COP is 0.38 under available working conditions. The typical working conditions are a cooling water inlet temperature of 25 °C, a chilled fluid inlet temperature of −10 °C and exhaust gas inlet temperature of 550 °C. Through the analysis of the perdition results, some conclusions can be drawn for this work as follows:

(1) The double heat pipe type adsorber can solve the problem of corrosion between sea water and steel adsorber in ammonia system;
(2) This novel structure of adsorber can improve the heat transfer performance in the adsorber. The adsorber could be heated up or cooled down from 118 to 43 °C in 12 min. It costs only half-cycle time of split heat pipe type adsorber and the temperature variation range is even larger than in split heat pipe type adsorber.
(3) It also simplifies the adsorber structure and decreases the cost because there are only five valves in the whole system.
(4) When the exhaust gas temperature is 550 °C, the cooling water temperature is 25 °C, the inlet and outlet chilled water are at −10 and −15.6 °C, respectively; the simulation results show that the cooling power and COP of this adsorption system are 5.1 kW and 0.38, respectively.
(5) For a better cooling power and COP of the system, a heating/cooling time of 720 s and mass recovery time of 60 s are recommended.
(6) The mass recovery process has a great influence on the adsorber temperature and chilling fluid temperature.

Acknowledgments

This work is supported by National Science Fund of China under Contract No. 50676060. The authors also thank the help of Dr. R.G. Oliveira in simulation and adsorption rate equation works.

References

[1] Wang RZ, Wu JY, Dai YJ, Wang W, Jiang ZS. Adsorption refrigeration. Beijing, China: Machine Press; 2002.
[2] Meunier F. Solid sorption: an alternative to CFCs. Heat Recov Syst CHP 1993;13(4):289–95.
[3] Meunier F. Second law analysis of a solid adsorption heat pump operating on reversible cascade cycles: application to the zeolite-water pair. J Heat Recovery Syst 1985;5:133–41.
[4] Meunier F. Solid sorption heat powered cycles for cooling and heat pumping applications. Appl Therm Eng 1998;18:715–29.
[5] Vasiliev LL, Mishkinis DA, Antukh AA, Vasiliev Jr, LL. New solid sorption refrigerator. In: Proceedings of the International Conference on Energy and Environment, ICEE, Shanghai, China, 1998.
[6] Vasiliev LL, Mishkinis DA, Antukh AA, Vasiliev Jr LL. Solar–gas solid sorption heat pump. Appl Therm Eng 2001;21:573–83.
[7] Vasiliev LL. Sorption refrigerators with heat pipe thermal control. In: Proceedings of ICCR'2003, Zhejinag, Hangzhou. p. 405–15.
[8] Wang RZ. Efficient adsorption refrigerators integrated with heat pipes. Appl Therm Eng, in press, doi:10.1016/j.applthermaleng.2006.02.028.
[9] Wang LW, Wang RZ, Wu JY, Xia ZZ, Wang K. A new type adsorber for adsorption ice maker on fishing boats. Energy Convers Manage 2005;46:2301–16.
[10] Wang LW, Wang RZ, Lu ZS. Split heat pipe type compound adsorption ice making test unit for fishing boats. Int J Refrig 2006.
[11] Wang LW, Wang RZ, Lu ZS, Chen CJ. Studies on split heat pipe type adsorption ice-making test unit for fishing boats: choice of heat pipe medium and experiments under unsteady heating sources. Energy Convers Manage 2006;47:2081–91.
[12] Lu ZS, Wang RZ, Wang LW, Chen CJ. Performance analysis of an adsorption refrigerator using activated carbon in a compound adsorbent. Carbon 2005;44:747–52.
[13] Wang DC, Xia ZZ, Wu JY, Wang RZ, Zhai H, Dou WD. Study of a novel silica gel–water adsorption chiller. Part I. Design and performance prediction. Int J Refrig 2005;28:1073–83.

[14] Wang DC, Wu JY, Xia ZZ, Zhai H, Wang RZ, Dou WD. Study of a novel silica gel–water adsorption chiller. Part II. Experimental study. Int J Refrig 2005;28:1084–91.
[15] Yang GZ, Xia ZZ, Wang RZ, Keletigui D, Wang DC, Dong ZH, et al. Research on a compact adsorption room air conditioner. Energy Convers Manage 2006;47:2167–77.
[16] Wang K, Wu JY, Wang RZ, Wang LW. Composite adsorbent of $CaCl_2$ and expanded graphite for adsorption ice maker on fishing boats. Int J Refrig 2006;29:199–210.
[17] Wang K, Wu JY, Wang RZ, Wang LW. Effective thermal conductivity of expanded graphite–$CaCl_2$ composite adsorbent for chemical adsorption chillers. Energy Convers Manage 2006;47: 1902–12.
[18] Oliveira RG, Wang RZ. A consolidated calcium chloride–expanded graphite compound for use in sorption refrigeration systems. Carbon 2007;45(2):390–6.
[19] Oliveira RG. Consolidated composite reactive bed for refrigeration sorption system. Post-doctoral final report, Shanghai Jiaotong University, 2006.
[20] Wang RZ, Wang QB. Adsorption mechanism and improvement of adsorption equation for adsorption refrigeration pairs. Int J Energy Res 1999;23:887–98.
[21] Wang LW. Adsorption performances, adsorption mechanisms and application of efficient compound adsorbent for efficient adsorption refrigeration driven by waste heat. PhD thesis, Shanghai Jiaotong University, 2006.